International Journal of Multiphase Flow 133 (2020) 103448

Contents lists available at ScienceDirect

International Journal of Multiphase Flow

journal homepage: www.elsevier.com/locate/ijmulflow

Insights on the morphology of air-assisted breakup of urea-water-solution sprays for varying surface tension

Aniket P. Kulkarni*, Thanos Megaritis, Lionel Christopher Ganippa

College of Engineering Design and Physical Sciences, Brunel University London, Uxbridge UB8 3PH, United Kingdom

ARTICLE INFO

Article history:
Received 12 March 2020
Revised 11 August 2020
Accepted 2 September 2020
Available online 5 September 2020

Keywords:
Urea-water solution
Selective catalytic reduction (SCR) system
High-speed visualization
Atomization
Drop-Size distribution
Surface tension

ABSTRACT

The efficacy of NO_x reduction in diesel engines is mainly dependent on how uniformly urea-water solutions (UWS) are dispersed onto the catalyst surface of the Selective Catalytic Reduction (SCR) systems. The urea-based SCR systems also suffer drawbacks due to the formation of urea deposits onto the walls of after-treatment devices due to poor atomization characteristics of UWS. In this work, the impact of lowering the surface tension of UWS on the morphology of UWS sprays was explored using high-speed shadowgraph imaging techniques. The surface tension of UWS was lowered by adding surfactants; two surfactants viz., Sodium Dodecyl Sulfate (SDS) and Dodecyl-Dimethyl-Amine-oxide (DDA) were considered in this investigation. The surface tension of UWS was reduced to a maximum from 73.7 to 30.2 mN/m and 39.8 mN/m with the addition of DDA and SDS respectively at 75% of its respective Critical Micelle Concentration (CMC) in UWS. Even at a very low-pressure difference of 500 mbar of co-flowing air, the surfactant-added UWS tends to break-up relatively closer to the nozzle tip due to flapping-induced bag breakup, which improved its drop-size distribution. Under a relatively higher pressure difference of 2000 mbar of co-flow atomizing air, the liquid breakup was mostly due to surface stripping in surfactant-added UWS sprays that generated a large number of fine droplets. The image analyses of sprays were performed at far downstream locations from the nozzle to quantify the variations of their droplet-sizes caused by varying the surface tension of UWS. The surfactants added UWS sprays revealed a considerably narrower drop-size distribution by up to 43% compared to UWS sprays under high-pressure conditions, and this was due to a combination of flapping-induced bag breakup, surface stripping and secondary atomization of big droplets caused by reducing the surface tension of UWS. Reducing the surface tension of UWS has the potential to improve NO_x reduction in SCR systems due to the reduction in droplet sizes of UWS sprays and also to reduce the formation of urea deposits.

1. Introduction

The nature of fuel to energy conversion process in various combustion systems generate many harmful emissions including soot and nitric oxides (NO_x). After-treatment devices are commonly used to achieve the simultaneous reduction of both soot and NO_x emissions (Guan et al., 2014). The abatement of NO_x is effectively achieved by using selective catalytic reduction (SCR) systems (Guan et al., 2014; Birkhold et al., 2006). This method relies on the injection of urea water solution (UWS, 32.5% urea by weight) into the exhaust gases (Birkhold et al., 2006; Ebrahimian et al., 2012). The injected UWS evaporates due to heat available in the exhaust gases and undergoes a series of chemical processes such as hydrolysis and thermolysis to generate ammonia vapour which acts as a reducing agent to decompose NO_x in the presence of a catalyst (Guan et al., 2014; Spiteri et al., 2015; Varna et al., 2015). Many efforts have been made to improve the performance of SCR systems to achieve better NO_x conversion efficiency and to minimize impingement of UWS droplets on the walls of the SCR systems. These efforts include use of mixer configurations (Oh and Lee, 2014; Lecompte et al., 2014), which enhances the mixing of UWS with exhaust gases and this improves the NO_x conversion efficiency of the SCR system (Guan et al., 2014). The mixing process is mainly governed by atomization characteristics of UWS sprays (Guan et al., 2014; Varna et al., 2015; Wong et al., 2004; Payri et al., 2019a). Moreover, poorly atomized and non-vaporized droplets from UWS spray may impinge on the internal surfaces of the SCR system which leads to urea residues (Spiteri et al., 2015; Liao et al., 2017; Huang et al., 2020; Koebel et al., 2000; Dörnhöfer et al., 2020; Eggers and Villermaux, 2008). Thus, it is impor-

* Corresponding author.
E-mail address: aniket.kulkarni@brunel.ac.uk (Aniket P. Kulkarni).

https://doi.org/10.1016/j.ijmultiphaseflow.2020.103448

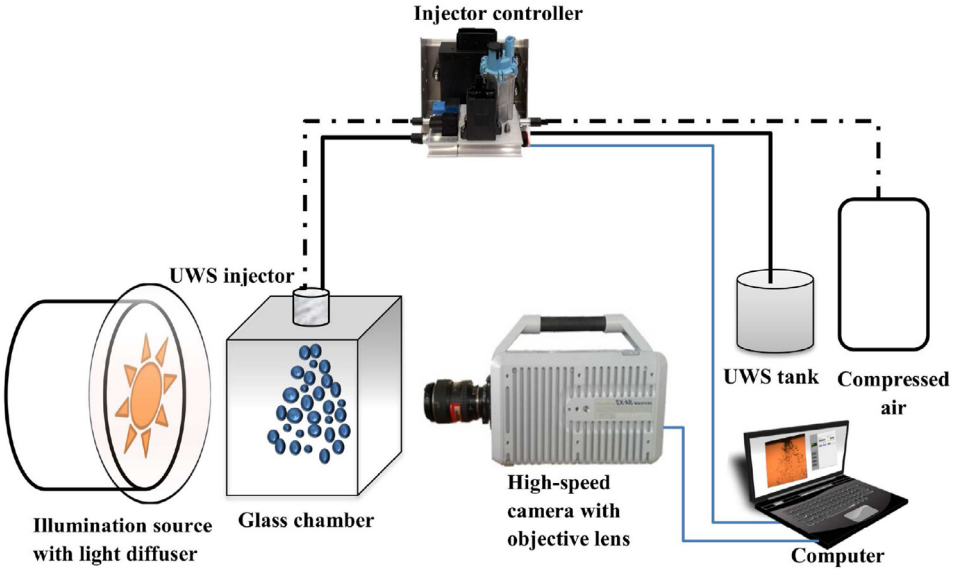

Fig. 1. Schematic of experimental setup used to study the effect of surface tension on breakup processes and atomization characteristics of UWS sprays using high-speed shadowgraph imaging.

tant to study atomization characteristics of UWS sprays to achieve improved NO_x conversion efficiency with minimum wall impingement.

The spray characteristics of UWS have been widely studied under non-evaporative and evaporative cross-flow conditions (Varna et al., 2015; Payri et al., 2019a; Liao et al., 2017; Payri et al., 2019b; Shi et al., 2013; Kapusta et al., 2019; Kapusta, 2017). Varna et al. (2015) studied UWS sprays from a pressure-driven atomizer at 9 bar injection pressure for different velocities of cross-flow; wall-hitting was observed under low cross-flow velocities. The effect of injection angle on the mixing length in an SCR system was studied for a pressure-driven atomizer (Shi et al., 2013). It was found that orthogonal injection to exhaust flow leads to a shorter mixing length. Payri et al. (2019a,b) studied the effect of injection pressure and temperature of cross-flow using a pressure-driven atomizer on the size and velocity distributions of UWS droplets. They found that droplet velocity in cross flow increases with high gas temperatures due to change in density of gas flow. They concluded that smaller droplets with higher droplet velocities can be produced at high temperatures of cross-flow (Payri et al., 2019a; 2019b), these observations are consistent with those reported in (Postrioti et al., 2015; Needham et al., 2012). Spiteri et al. (2015) compared spray-air interactions for air-assisted and pressure-driven atomizers under cross-flow conditions, the UWS sprays from pressure-driven atomizer are least affected by cross-flow velocities and this leads to wall-impingement. On the other hand, air-assisted atomizers produced droplets of smaller Sauter Mean Diameter (SMD), resulting in better mixing of UWS and exhaust gases. Thus, air-assisted atomization strategy has gained attraction for atomization of UWS in SCR systems (Spiteri et al., 2015; Zheng, 2017). Recently, it was demonstrated that atomization of UWS can also be improved with the help of electrostatic force (Pratama et al., 2019). Many studies have employed Phase Doppler Interferometry (Varna et al., 2015; Liao et al., 2017; Pratama et al., 2019; Shi et al., 2013) or back-light illumination measurements (Payri et al., 2019a; 2019b; Lieber et al., 2019) for characterization of UWS sprays. Most of these studies have focused on droplet SMD and distributions of droplet size and velocity. It was reported that UWS droplets below 20 µm can completely entrain or evaporate in engine-exhaust like situations (Liao et al., 2017; Liao, 2017). The impingement rate of UWS droplets was higher with large droplets and, droplets larger than 90 µm droplet diameter are likely to impinge on walls of the SCR system (Liao et al., 2017; Liao, 2017). These larger droplets may also affect NO_x conversion efficiency. Thus, it important to reduce the presence of bigger size droplets (i.e. droplets larger than 90 µm droplet diameter). This observation highlights the need of narrower drop-size distributions in UWS sprays for effective NO_x conversion in SCR systems with minimum wall residues. This can be achieved by varying the physical properties of UWS, which might improve its atomization characteristics. The physical properties of UWS can be altered by adding surfactants to improve atomization (Lecompte et al., 2014; Ayoub et al., 2011; Wasow and Strutz, 2015; Ayyappan et al., 2015; Tareq et al., 2020; Kooij et al., 2018; Sijs et al., 2019; Sijs and Bonn, 2020). Ayoub et al. (2011) studied the effect of using surfactants as additives to improve NO_x conversion efficiency in SCR systems. Various surfactants viz., dodecyldimethylamine oxide (DDA), Stearyl trimethyl ammonium chloride, Sodium lauryl ether sulfate (SLES) and Sodium dodecyl sulfate (SDS) were considered. It was reported that the addition of surfactants to UWS improved NO_x conversion efficiency, and better reduction of NO_x was achieved with anionic surfactants such as SDS and SLES in engines (Ayoub et al., 2011). However, spray characteristics were not explored in their work. The alcohol ethoxylates-based surfactants were also studied to improve drop-sizes in UWS sprays (Wasow and Strutz, 2015). It was reported that surface tension of UWS reduced from 67 to 28.87 mN/m while, droplet sizes were reduced upto 75% using these surfactants. Surfactants have also been used to reduce wall hitting in SCR systems due to improved atomization characteristics of UWS sprays. Ayyappan et al. (2015) used Formaldehyde-based additive to reduce urea wall deposit and, achieved up to a maximum of 77.1% reduction. These observations corroborate with the findings of Lecompte et al. (2014). Thus, NO_x conversion efficiency and wall residues can be controlled simultaneously by using surfactants as additives. The improvement in NO_x conversion efficiency and decrease in wall impingement with surfactant-added UWS may be attributed to improved atomization characteristics of UWS sprays, resulting in smaller drop sizes and narrower drop-size distributions. Narrower drop-size distribution helps to achieve better mixing due to smaller droplet diameters, and the absence of big droplets reduces wall-residues. The near-nozzle breakup also influences the

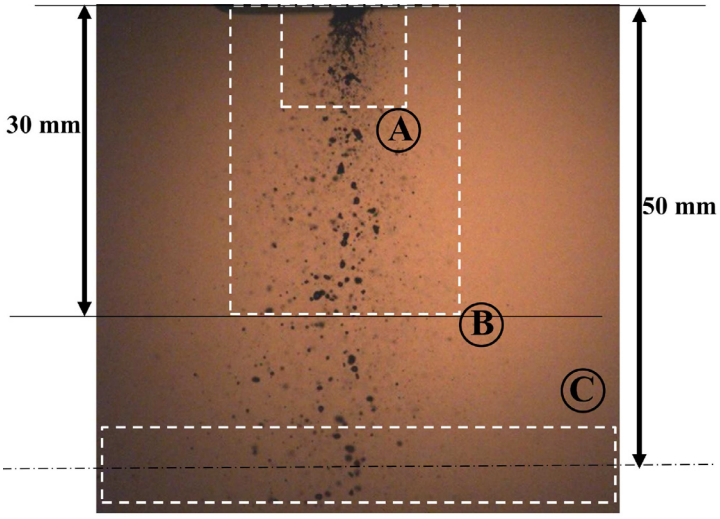

Fig. 2. Schematic representation of measurement locations used to obtain atomization characteristics. High-speed imaging technique allowed to capture breakup processes of UWS air-assisted sprays. The field of view of the measurements (width × height) are: Ⓐ - 5.3 mm × 3.5 mm; Ⓑ - 15 mm × 30 mm; and Ⓒ - 20 mm × 3.5 mm.

resultant drop size distributions in the far-field region of the UWS sprays. Thus, it is important to understand the breakup processes occurring in the near-nozzle region of the air-assisted UWS sprays, particularly for varying surface tension values of UWS as not much work has been done to explore the mechanisms that influence near-nozzle breakup.

In this work, the effect of adding surfactants on the breakup processes of air-assisted UWS spray have been explored at various pressures of the atomizing air. The breakup processes occurring in the near-nozzle region, global spray structure and drop-size distributions of UWS and surfactant-added UWS sprays were studied using the high-speed shadowgraphy method.

2. Experimental setup and methods

2.1. Experimental setup and back-light imaging

The schematic of the experimental setup is shown in Fig. 1. Air-assisted spray of UWS was injected into a non-reactive, quiescent glass chamber under ambient conditions (i.e. ambient gas temperature of 20 °C and atmospheric pressure conditions). The spray was back-illuminated using an LED light source and shadowgraph images were acquired using a high-speed camera (Photron, SA X-2) equipped with Tokina macro 100, F2.8 objective lens of 100 mm focal length. The imaging system was moved to different positions to study global spray structure, near-nozzle and drop-sizing as shown in Fig. 2. The breakup processes occurring in the near-nozzle region Ⓐ were captured in a window of 5.3 mm × 3.5 mm (width × height) just below the injector tip at 168,000 frames per second (fps) and a shutter speed of 0.29 µs. The adopted high frame rate and small shutter speed enabled to capture temporal evolutions and breakup mechanisms causing the near-nozzle spray

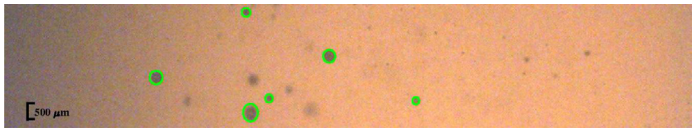

Fig. 3. An example of an instantaneous drop-sizing image in UWS spray at ΔP = 500 mbar. Only circled droplets were considered in drop-size distributions.

breakup processes. Global spray structures in region Ⓑ were captured at 16,000 fps with a field of view of 15 mm × 30 mm at an exposure of 0.29 μs. Drop-sizing measurements were carried out in a window of 20 mm × 3.5 mm at 67,500 fps in region Ⓒ. The drop-sizing measurements were performed at 50 mm below the injector tip to ensure that most of the atomization processes have occurred and most of the droplets were spherical. The shadow images of the droplets were analyzed using an in-house developed MATLAB code for drop-size measurements. The images were pre-processed using the median filter and image subtraction. A binary image was then obtained using the subtracted image and global thresholding. Image segmentation was performed to extract area of the droplets. Out-of-focus droplets and droplets with sphericity less than 0.8 were neglected for reliable drop-sizing (Blaisot and Yon, 2005; Kulkarni and Deshmukh, 2017). Same droplets that appeared in a sequence of frames due to high-speed imaging were filtered using residence time calculated for every operating condition. Statistically sufficient number of droplets (more than 6000 droplets) are ensured in drop-size distribution calculations. Uncertainty in drop-size measurements was estimated to be less than 9.7%. The resolution of drop-size images was 22.2 µm per pixel, thus droplets with diameter less than 80 µm were neglected to avoid diffraction limit of the optical system and for reliable drop-

Table 1
Details of optical setup used in high-speed shadowgraphy.

Type of measurements	Camera and objective lens	fps	Shutter speed (exposure)	Pixel resolution
Global spray structure	Photron, SA X-2; Tokina macro 100, F2.8	16,000	0.29 µs	768 x 1024
Near-field visualization		168,000	0.29 µs	256 x 184
Drop-sizing		67,500	0.29 µs	1024 x 184

Table 2
Surface tension values of the test liquids at room temperature.

	DDA			SDS			UWS
Concentration (% of cmc)	25	50	75	25	50	75	
Surface tension (mN/m)	40.84	34.26	30.20	53.87	43.00	39.80	73.70
Standard deviation (mN/m)	1.59	0.30	0.95	0.30	0.76	0.17	1.18
Mean standard error (%)	1.30	0.31	1.29	0.19	0.62	0.18	0.54

Table 3
Dynamic viscosity and density of the test liquids at room temperature.

	DDA			SDS			UWS
Concentration (% of cmc)	25	50	75	25	50	75	
Dynamic viscosity (mPa.s)	1.41	1.45	1.42	1.44	1.44	1.75	1.41
Density (kg/m^3)	1058.9	1078.4	1070.3	1055.8	1063.11	1061.8	1066.3

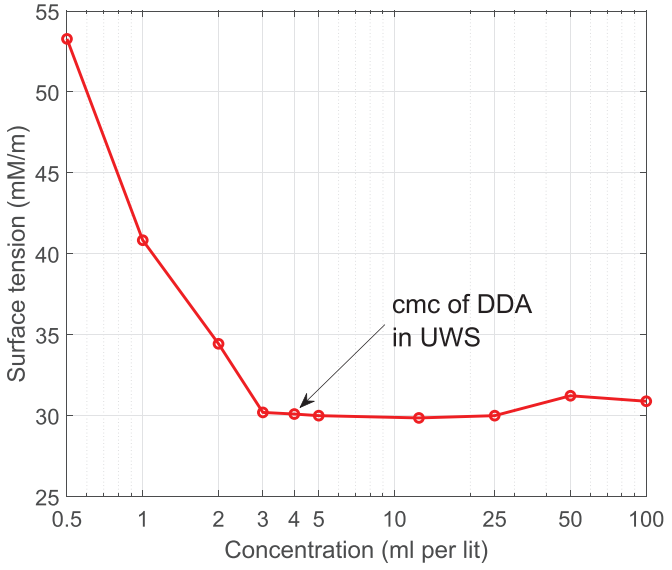

Fig. 4. Surface tension values of UWS for various concentrations of DDA surfactant. Critical micelle concentration (cmc) of DDA in UWS was determined as 4 ml per liter using the pendant drop method of surface tension measurement.

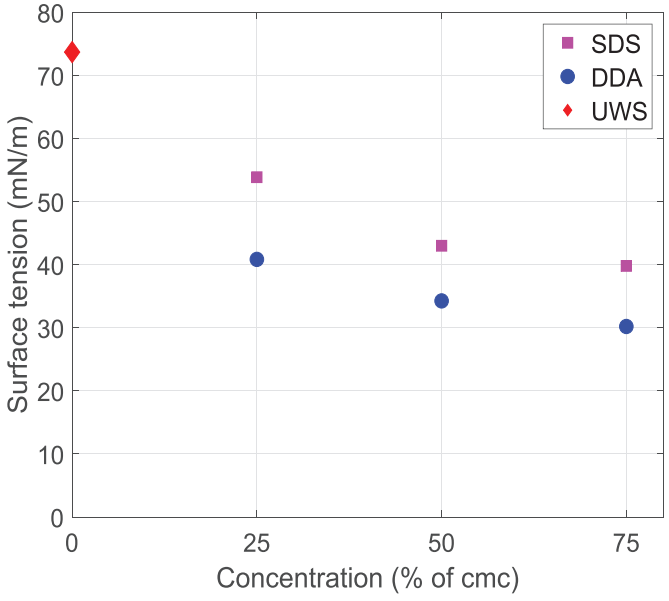

Fig. 5. Comparison of surface tension values of surfactants added UWS at various concentrations and UWS without surfactant. Surface tension of UWS reduced from 73.7 to 30.2 mN/m with addition of DDA surfactant at concentration of 75% of cmc in UWS.

size measurements. This also ensured that the droplets larger than 90 µm are captured in the drop-size distributions, which may cause wall-hitting. Fig. 3 shows an example of the images obtained and droplets considered for determining the drop-size distribution. Further details of the optical setup used in the present work are summarized in Table 1.

2.2. Preparation of test liquids and measurements of physical properties

In this subsection, methods adopted to prepare test liquids and details on measurements of physical properties of the test liquids (surface tension, dynamic viscosity and density) have been provided.

2.2.1. Preparation of test liquids

Commercially available urea-water solution (UWS, 32.5% urea in water on mass basis) along with two surfactants, Sodium dodecyl sulfate (SDS) and N,N, Dimethyldodecylamine N-oxide (DDA), were used in the present work. These surfactants were selected based on the past studies which reported improvements in NO_x conversion efficiency while using these surfactants in urea-SCR systems (Lecompte et al., 2014; Ayoub et al., 2011; Wasow and Strutz, 2015). The surfactants were added to UWS in 25%, 50% and 75% of their respective critical micelle concentration (cmc) values. The cmc value can be referred to as the concentration of surfactants above which micelles are formed, and surface tension reduces marginally or remains unchanged with the further addition of the surfactant. The cmc values of SDS and DDA surfactants are well-documented for water. However, it was observed that the cmc values are different for the binary liquids including UWS (Ayoub et al., 2011). The cmc value of SDS in UWS was obtained from literature (Ruiz, 1999) as 6 µmol per litre. The cmc value for DDA in UWS was 4 ml per litre and this was determined experimentally by measuring the surface tension of the surfactant-added UWS solutions at various concentrations as shown in Fig. 4.

2.2.2. Physical properties of the test liquids

The physical properties of the test liquids were measured at room temperature of 20 °C. The surface tension measurements were carried out using pendent-drop method (First Ten Angstroms, FTA100), the measurements were calibrated using deionized water as a standard liquid. Minimum ten measurements were performed at each test condition, and standard deviation and mean standard error was calculated as shown in Table 2. The maximum mean standard error in the surface tension measurements

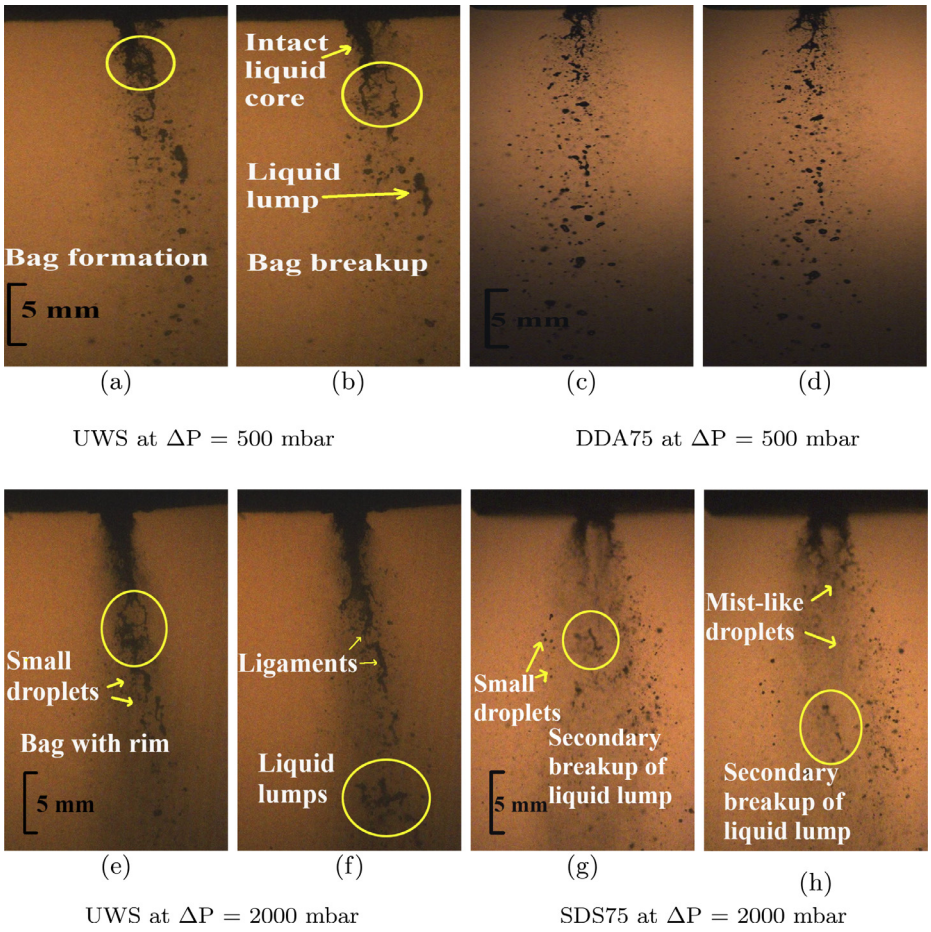

Fig. 6. Global structure of sprays from UWS, SDS 75 and DDA 75 at ΔP = 500 mbar and 2000 conditions at random time intervals. The UWS sprays showed poor liquid distribution compared to surfactant added UWS sprays. Bag breakup was observed in UWS sprays. Liquid lumps were observed in UWS sprays even at high ΔP condition. Whereas, secondary breakup of big droplets improved global structure of surfactant added UWS sprays.

was less than 1.3%. The effect of addition of SDS and DDA surfactants to UWS in various concentrations (25, 50 and 75% of cmc) on surface tension values have been compared in Fig. 5. Surface tension of UWS reduced significantly with addition of the surfactants to UWS and a minimum value of 30.2 mN/m was observed with DDA surfactant with the concentration of 75% (DDA75). Dynamic viscosity was measured using a rolling ball viscometer (Anton Paar, AMVn). Density was determined using a high-precision weighing machine. It was observed that the addition of surfactants has marginal influence on dynamic viscosity and density of the UWS. Physical properties of the test liquids are summarized in Table 3.

2.3. Test conditions

The experiments were carried out using UWS and six solutions of surfactant-added UWS. Three concentrations were used to form SDS25, SDS50 and SDS75 using 25, 50 and 75% of cmc value of SDS surfactant in UWS, respectively. Similarly, DDA25, DDA50 and DDA75 were prepared using DDA surfactant in UWS. The spray experiments were carried out at a fixed liquid flow rate of 1000 g/hr and different gauge pressures (ΔP) of atomizing air at 500, 1000, 1500 and 2000 mbar; the parameters of spray injection were controlled using a commercial controller(Albonair, 2017). Gas to liquid mass ratios (GLR) at these ΔP conditions are 0.68, 1.02, 1.35 and 1.69, respectively. Air-assisted UWS spray was injected using a single-hole, externally mixed injector with an injection duration of around 40 ms, having a diameter of 1 mm (i.e. d_{liquid} =1 mm)

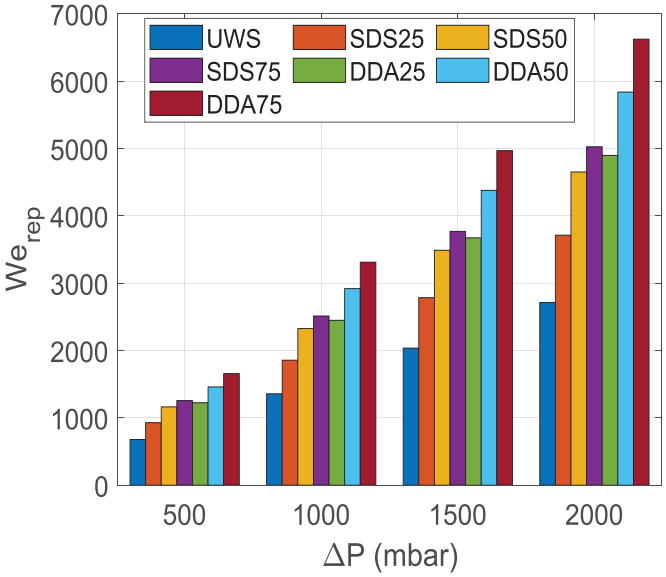

Fig. 7. We_{rep} values of surfactant-added UWS solutions at various ΔP conditions.

through which liquid was injected into the continuous coaxial jet of swirling atomizing air. The study, including the spray experiments and measurements of the physical properties, was conducted under ambient pressure and temperature conditions (i.e. atmospheric pressure and 20 °C) with ambient temperature of UWS.

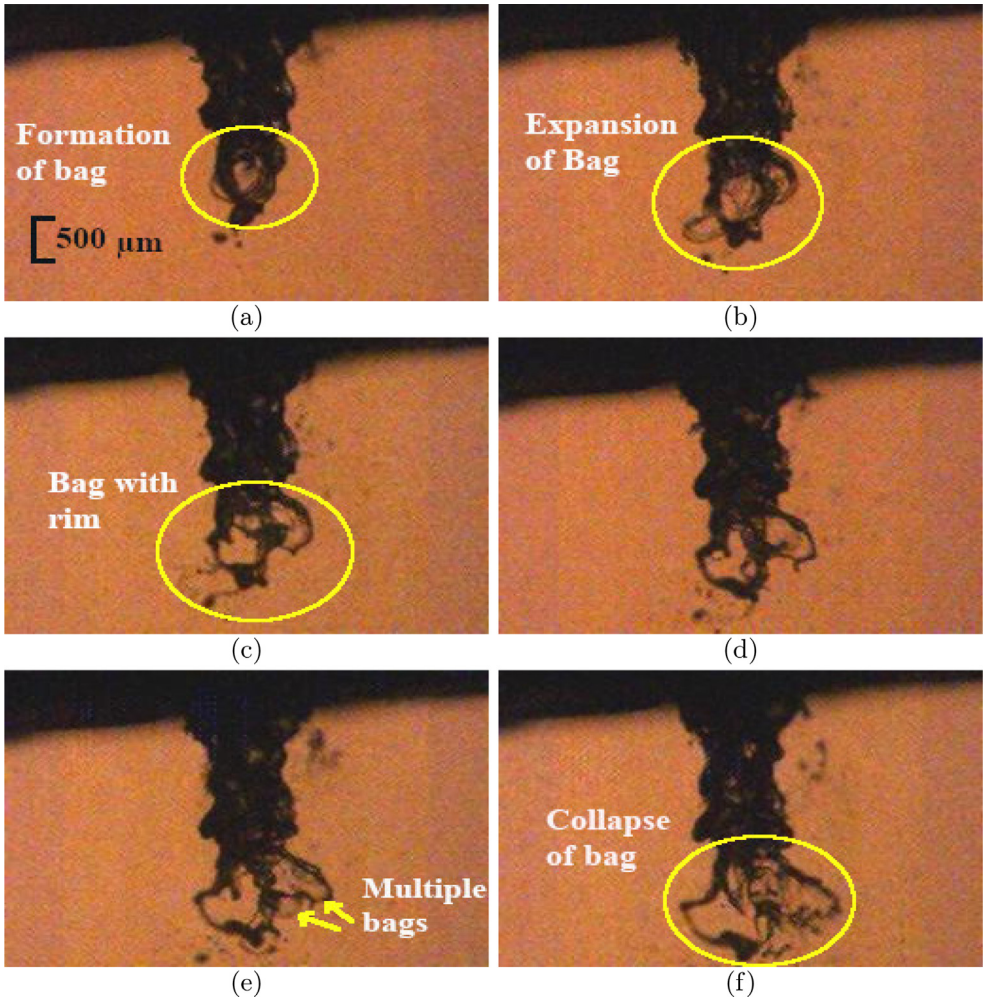

Fig. 8. Breakup processes in UWS spray at $\Delta P = 500$ mbar condition at random time intervals. Bag breakup was observed at the tip of an intact liquid core.

3. Results and discussion

Addition of surfactants in various concentrations reduced surface tension of UWS significantly. The impact of surface tension on breakup processes of the air-assisted sprays of UWS was studied at various gauge pressures of atomizing air. The air-assisted breakup processes and spray characteristics are different for UWS and for surfactant doped UWS.

3.1. Global spray structure

In this subsection, global spray structures of UWS and surfactant-added UWS sprays were studied at 500 and 2000 mbar conditions. Fig. 6 compares global structure of UWS spray with that of surfactant-added UWS sprays at ΔP of 500 and 2000 mbar conditions. The global structures of the surfactant added UWS sprays were significantly different under all ΔP conditions compared to UWS due to a large difference in surface tension values. Addition of surfactants improved the breakup of UWS jet, showing a better distribution of liquid at 500 mbar condition as shown in Figs. 6(c) and 6(d) for DDA75 sprays. The UWS sprays have longer intact liquid core compared to that of surfactant-added UWS sprays suggesting poor atomization of UWS. Bag formation was also observed downstream of the intact liquid core for UWS, as highlighted in Figs. 6(a) and 6(b). The breakup of these bags resulted in a combination of small and big droplets from rupture of the stretched bag and its rim. Fragmentation of rim also resulted in ligament-like structures and relatively large lumps of liquid due to impact and coalition of droplets of varying sizes transported randomly at different momentum. As the pressure of swirling coflow of air increases, the breakup due to Kelvin-Helmholtz instability enhances, which generates a large number of small droplets of UWS as shown in Fig. 6(e). Significantly high number of small and mist-like droplets were observed for surfactant-added UWS sprays showing better atomization as shown in Figs. 6(g) and 6(h). These small droplets might have resulted from stripping of the liquid surface due to low surface tension of surfactant-added UWS and high relative velocity between the liquid jet and swirling coflow of atomizing air jet at high ΔP conditions (Lasheras et al., 1998; Guildenbecher et al., 2009; Varga et al., 2003; Zhao et al., 2018). Even at high $\Delta P = 2000$ mbar condition, bag formation was observed which resulted in few liquid lumps and big droplets, originated from the rim of bags for UWS sprays, as observed in Fig. 6(f). These big droplets could not undergo further secondary breakup due to high surface tension of UWS. Addition of surfactants reduced surface tension of UWS, this favoured the secondary breakup of big droplets and liquid lumps as can be seen in Figs. 6(g) and 6(h). Hence, surfactant-added UWS sprays showed more uniformly distributed droplets along with very less number of big droplets at high gas pressure conditions.

Thus, better atomization was achieved through the addition of the surfactant in UWS and this was due to the combination of

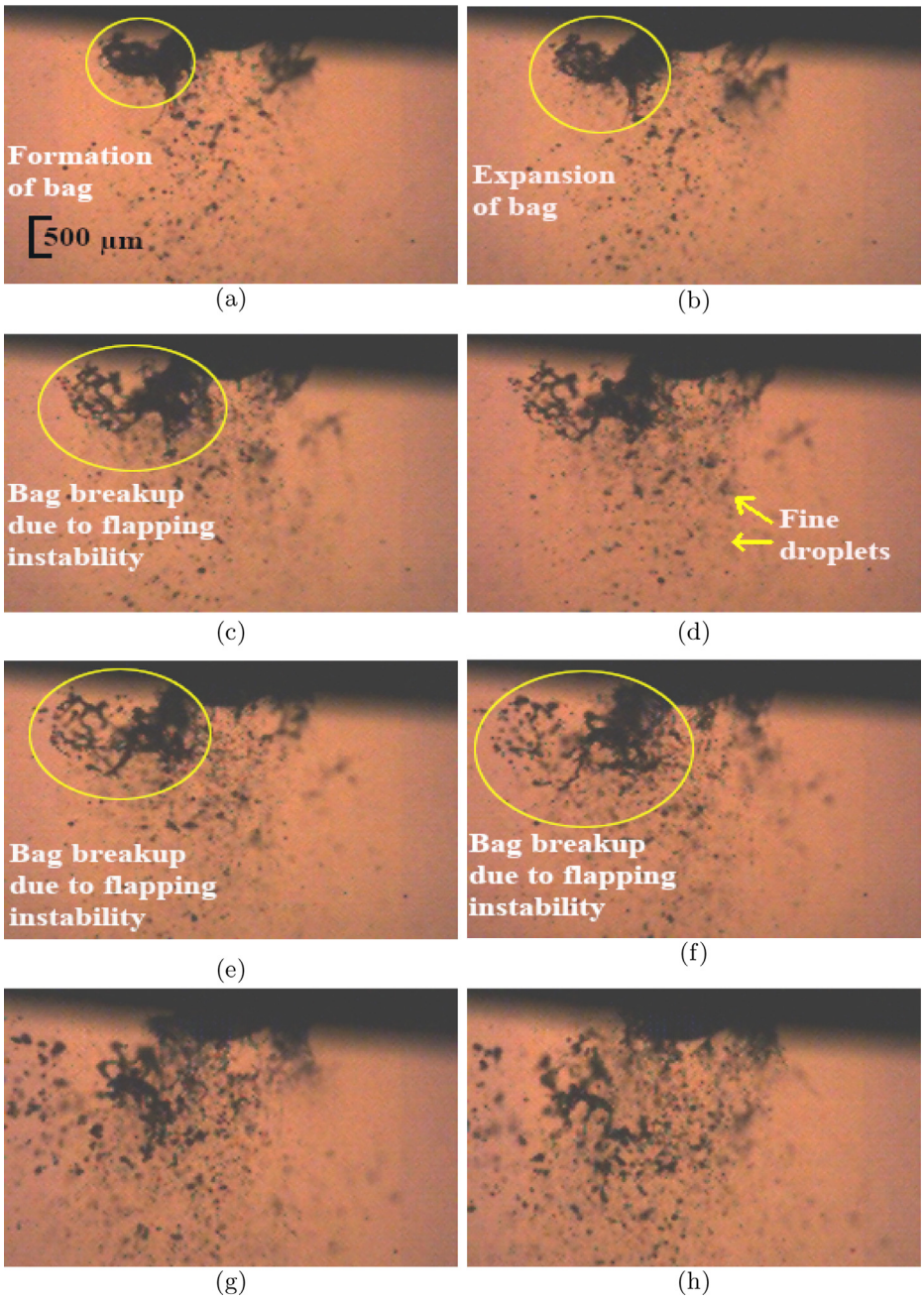

Fig. 9. Breakup processes in DDA 50 sprays at $\Delta P = 500$ mbar condition with $We_{rep} = 1459.43$ at random time intervals. Flapping-induced bag breakup was the predominant mode of jet breakup. This mode of breakup improved atomization of UWS even at low ΔP conditions with the addition of surfactants.

droplet stripping and secondary atomization of big droplets at high air pressures in surfactant-added UWS sprays.

3.2. Effect of surfactants on breakup processes in near-nozzle region

This section presents the breakup processes occurring in near-nozzle region of air-assisted UWS sprays. Primary breakup processes were studied to reveal the effect of addition of surfactants and atomizing air pressures (ΔP). The combined effect of ΔP and surface tension of UWS on liquid jet breakup processes can be evaluated by using a dimensionless representative We number (We_{rep}) for each condition.

Aerodynamic Weber number can be defined as :

$$We = \frac{Inertia\ forces\ of\ air}{Surface\ tension\ forces\ of\ liquid} \quad (1)$$

As inertial forces due to swirling air-stream are proportional to ΔP, according Bernoulli's equation:

$$We \propto \frac{\Delta P}{\sigma_{liquid}} \cdot d_{liquid} \quad (2)$$

Thus, representative Weber number (We_{rep}) can be defined in terms of ΔP and σ_{liquid} for a given liquid jet diameter and expressed as:

$$We_{rep} \approx \frac{\Delta P}{\sigma_{liquid}} \cdot d_{liquid} \quad (3)$$

Fig. 7 shows the calculated values of We_{rep} for UWS and various surfactant-added UWS at various ΔP conditions. Various breakup processes, such as bag breakup, flapping-induced bag breakup, surface-stripping and secondary breakup of big droplets, were all observed in UWS sprays and surfactant added UWS sprays, these breakup processes can be related to We_{rep}. At

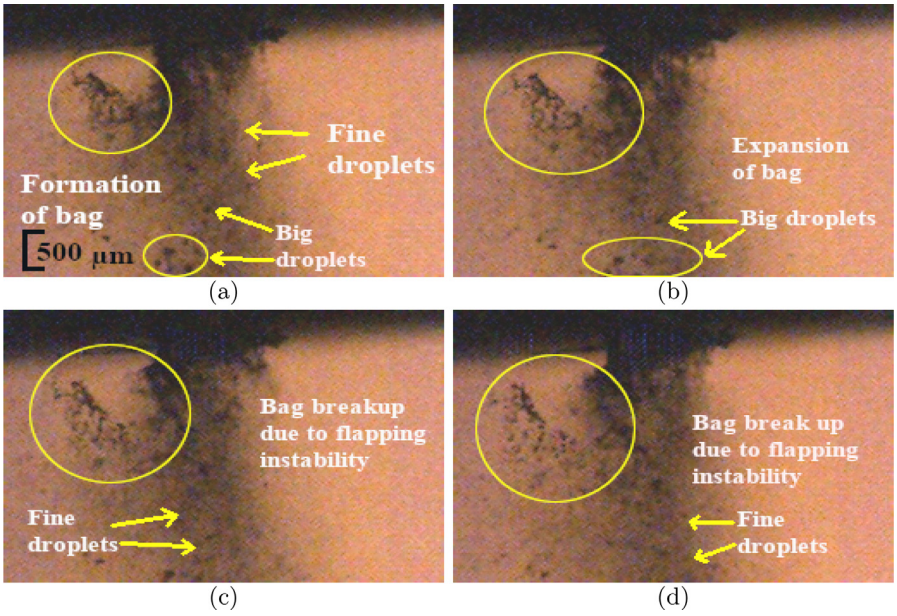

Fig. 10. Breakup processes in SDS 50 sprays at $\Delta P = 1500$ mbar condition with corresponding $We_{rep} = 3488.37$ at random time intervals. Flapping induced bag breakup and surface stripping both were predominant although few big droplets were also observed.

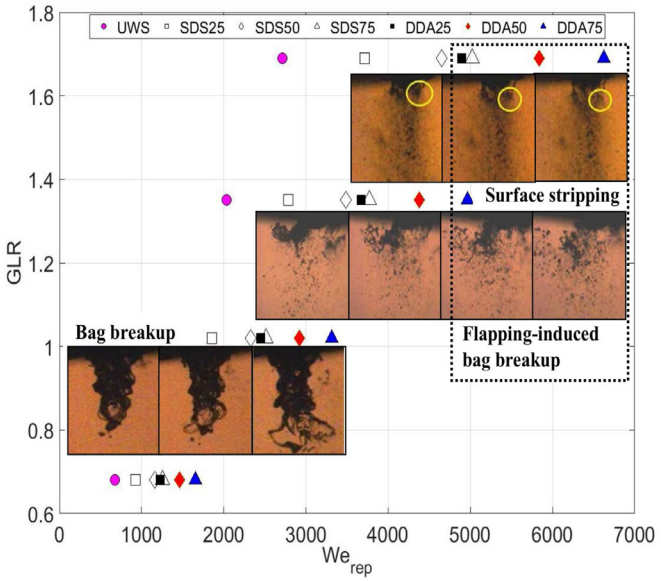

Fig. 11. Regime map of breakup processes observed in near-nozzle region of air-assisted UWS sprays for the range of We_{rep}. The combination of breakup processes improved jet breakup for We_{rep} more than 4966.89 as shown in the dotted region.

lower values of We_{rep}, bag formation in UWS jet was observed which expanded until the bag-like structure fragmented to form droplets (Guildenbecher et al., 2009; Zhao et al., 2018). In general, the bag breakup mode was observed over a range of We_{rep} between 678.43 and 1356.85 which corresponds to relatively higher surface tension and low ΔP conditions. In flapping-induced bag breakup mode, the bag-like structure oscillated about the axis of the liquid jet due to flapping instability, this type of breakup improved atomization of UWS even at low ΔP conditions. At higher values of We_{rep}, liquid droplets and ligaments were stripped-off from the surface of the UWS jet showing breakup of UWS jet due to surface stripping. This mode of jet breakup generated a large number of small, mist-like droplets (Lasheras et al., 1998; Guildenbecher et al., 2009). At high ΔP conditions, ligaments and big droplets formed in surfactant added UWS sprays experienced further secondary breakup showing secondary breakup of big droplets and ligaments.

Fig. 8 shows near-nozzle spray structure images of UWS spray at an atomizing air pressure of 500 mbar with the corresponding $We_{rep} = 678.43$. Breakup of the intact liquid core near the nozzle tip was initiated through bag breakup. The velocity and density gradients of the atomizing air and UWS triggers Kelvin-Helmholtz and Rayleigh Taylor instabilities, which leads to the formation of sheet along the surface of the liquid as shown in Figs. 8(a) and 8(b). The sheet was further expanded by the co-flowing atomizing air to form a bag-like structure due to competition between surface tension force of the liquid and aerodynamic force of the atomizing air as can be observed in Figs. 8(b) to 8(d). When the surface tension force was overcome by the aerodynamic force of the atomizing air, the bag-like structure fragments into droplets and ligaments from the rim of the bag structure became visible as seen in Figs. 8(e) and 8(f). Relatively larger size liquid droplets and ligaments were formed from the breakup of rim of the bag. These big droplets contain relatively more mass of liquid and may not evaporate completely in the SCR system due to its lower surface area available for evaporation.

Addition of surfactants increased We_{rep} due to the reduction in surface tension values as shown in Fig. 7. The length of intact liquid core was relatively short for surfactant added UWS sprays compared to that of UWS sprays at 500 mbar condition. Contribution to liquid jet breakup due to flapping instability was observed for We_{rep} more than 1459.43 and this has been presented in Fig 9 for DDA50 sprays at $\Delta P = 500$ mbar. In flapping-induced bag breakup mode, a bag was initially formed, and then expanded by the atomizing air as shown in Figs. 9(a) and 9(b). The bag then oscillates vibrantly before its sheet fragments due to flapping instability as observed in Figs. 9(c) to 9(f). Flapping of bag may be attributed to enhanced interaction between the bag structure and swirling atomizing air jet under reduced surface tension conditions amplified by the local recirculation zones. This observation corroborates the observations reported in the literature on liquid jet/sheet injected into swirling co-flow of air (Hopfinger and Lasheras, 1996; Matas and Cartellier, 2013; Rajamanickam and Basu, 2017), where flapping instability was induced by the central toroidal recirculation

zone in the swirling flow field. In this work, the observed flapping of the bag along with the jet improved liquid core breakup which generated atomized UWS spray as observed in Figs. 9(g) and 9(h). Further, the contribution of fine droplets stripping from liquid surface was marginal under this regime of breakup as can be shown in Fig. 9(d).

At higher values of We_{rep} (more than 3488.37), contribution of surface stripping was significantly high, along with small contribution of flapping-induced bag breakup, showing the presence of a large number of fine, mist-like droplets in Figs. 10(a) to 10(d) for SDS50 sprays at 1500 mbar condition. High velocity of atomizing air leads to stripping of droplets and ligaments from liquid surface due to strong shearing forces, thus fine mist-like droplets were observed at higher We_{rep} (Lasheras et al., 1998; Guildenbecher et al., 2009; Varga et al., 2003; Zhao et al., 2018). However, few big droplets could also be identified as can be seen in Figs. 10(a) and 10(b). Further at higher We_{rep} (more than 4966.89), secondary breakup of these bigger droplets were observed. This could be attributed to the combined effect of reduction in surface tension of UWS and higher velocities of atomizing gas that might have helped with breakup of these big droplets.

The observed breakup processes of UWS sprays have been summarized in a regime map for the range of We_{rep} and GLR as shown in Fig. 11. Distinct breakup processes (such as flapping-induced bag breakup, surface stripping and secondary atomization of big droplets) were observed in the near-nozzle region of UWS air-assisted sprays. It can be observed from the regime map that different processes were occurring simultaneously in the near-nozzle region of air-assisted UWS sprays. The combination of these breakup process was observed at high GLR conditions and We_{rep} more than 4966.89 which might generate finely atomized sprays of UWS. Thus, surface tension has strong influence on breakup processes in air-assisted UWS sprays.

3.3. Drop-size distributions

Drop-size distributions were obtained by analyzing the droplets in the window of 20 mm × 13.5 mm at a location of 50 mm below the injector tip as shown in Fig. 2. The drop-size distributions represent droplet probability against droplet diameter. Fig. 12 compares drop-size distributions of UWS sprays with those of surfactants-added UWS sprays at different ΔP conditions. A number of bigger size droplets of diameter more than 500 μm could be observed in the drop-size distributions of UWS sprays at low gas pressures (500 and 1000 mbar) as shown in Fig. 12(a). These droplets, though few in number, carry considerable liquid mass. These droplets are undesired as they may not evaporate completely in the SCR system and might lead to wall-hitting and formation of urea residues on the inner surface of SCR system. However, the number of big droplets in drop-size distributions of UWS sprays reduced at higher gas pressure conditions as can be seen in Fig. 12(c). Maximum droplet diameter in drop-size distri-

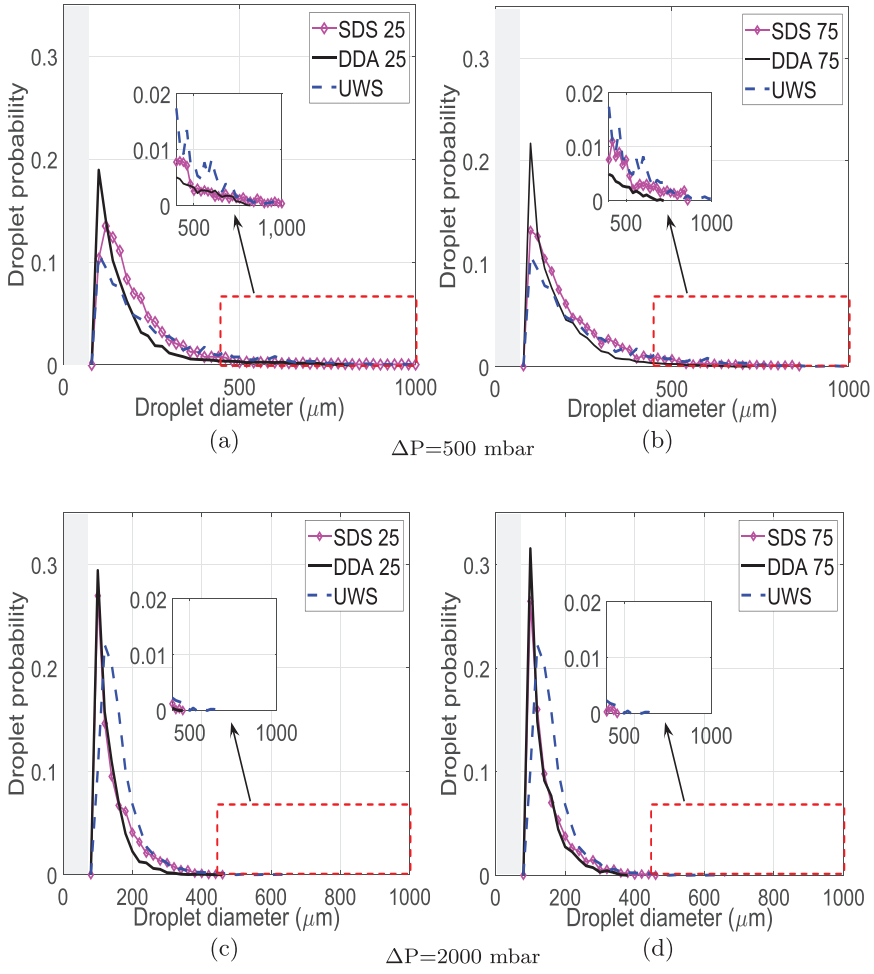

Fig. 12. Comparison between drop-size distributions from UWS sprays and those from surfactant added UWS sprays showing the effect of surfactant concentrations and ΔP. Drop-size distributions improved even at low ΔP conditions with addition of surfactants. Narrow drop-size distribution with most of the droplets smaller than 120 μm was observed with surfactant added UWS at high ΔP conditions.

bution (D_{max}) in UWS sprays decreased from 980 μm to 640 μm when ΔP was increased from 500 to 2000 mbar showing an effective droplet size reduction of up to 35%. This might be attributed to the combined effect of higher kinetic energy available in the atomizing air and improved breakup of UWS liquid jet due to flapping-induced bag breakup as discussed earlier.

Addition of surfactants to UWS significantly reduced surface tension of UWS. Thus, drop-size distributions of surfactant added-UWS sprays improved with a noticeable increase in the number of smaller size droplets at low gas pressures. Droplet probability of smaller size droplets (with droplet diameter < 100 μm) increased from 0.1 to 0.22 for DDA75 at ΔP = 500 mbar, as shown in Fig. 12(b). A similar observation was made at high ΔP conditions. The size of D_{max} decreased from 980 μm in UWS sprays to 660 μm in DDA75 sprays at 500 mbar condition showing a reduction up to 33% as shown in Fig. 12(b). The drop-size distributions became slightly narrower for surfactant-added UWS at low ΔP conditions as can be seen in Figs. 12(a) and 12(b)). This could be attributed to flapping-induced bag breakup observed in the near-nozzle spray structures at these conditions that might have produced narrower drop-size distributions. The drop-size distributions of surfactant-added UWS sprays significantly improved at high ΔP conditions with most of the droplets smaller than 120 μm droplet diameter as shown in Figs. 12(c) and 12(d). D_{max} also decreased from 640 μm in UWS sprays to 360 μm in DDA75 sprays at 2000 mbar condition showing a significant reduction of up to 43.7% as shown in Fig. 12(d). This can be attributed to the combination of breakup processes such as flapping-induced bag breakup, surface stripping and secondary breakup of big droplets as discussed in the previous sections. Overall, surfactant added-UWS sprays showed narrow drop-size distributions with most droplets of sizes smaller than 120 μm along with smaller D_{max} values. This suggests that faster evaporation (thus, shorter mixing length) and less wall impingement of UWS droplets in SCR systems might be obtained by using surfactant added-UWS sprays.

The findings summarize that atomization characteristics in air-assisted UWS sprays can be improved with the addition of the surfactants to UWS. In this work, addition of surfactants reduced surface tension of UWS considerably and improved breakup of air-assisted UWS spray through the combination of various breakup mechanisms. This resulted in narrower drop-size distributions with the higher number of smaller size droplets with larger surface to volume ratio. The associated increase in the droplet surface area due to lowering the surface tension of UWS will result in enhanced convective transfer of heat from surrounding hot exhaust gases to the droplets. This helps in faster evaporation of UWS droplets and hence, better mixing with the hot exhaust gases and better NO_x conversion efficiency. Further, reduction in droplet diameter will also help to minimize spray-wall interaction and formation of urea-residues in SCR systems. Overall, narrower drop-size distributions and thus, improved atomization of surfactant-added UWS sprays might help to enhance the performance of SCR systems with better NO_x conversion efficiency and lower urea-wall residues.

4. Conclusions

An experimental study was undertaken to study the effect of addition of surfactants in UWS on breakup morphology and atomization characteristics of air-assisted UWS sprays. Two surfactants (SDS and DDA) were used in the present work. Addition of surfactants significantly reduced surface tension of UWS from 73.7 to 30.2 mN/m. The investigation revealed distinct modes of breakup in UWS sprays for different ΔP and surface tension. UWS sprays showed poor near-nozzle atomization characteristics at high ΔP conditions with big droplets originating from inefficient breakup of dense and longer intact core due to aerodynamic forces unable to overcome high surface tension forces and rim during bag breakup process.

For surfactant added UWS, the aerodynamically induced flapping and associated bag-breakup effectively overcome surface tension forces and improved atomization of UWS even under low ΔP conditions. Significant contribution of surface stripping breakup was observed in surfactant-added UWS sprays at high ΔP conditions mainly due to high relative velocity and low surface tension of surfactant-added UWS. Global spray structure images of surfactant-added UWS sprays showed improved distribution of liquid. Narrow drop-size distributions along with significant reduction of up to 43.7% in D_{max} were observed in surfactant-added UWS sprays at high ΔP conditions which could be attributed to a combination of flapping-induced bag breakup, surface stripping and secondary breakup of big droplets. Thus, atomization characteristics of UWS sprays can be improved with addition of surfactants that might help to achieve better mixing, shorter mixing length and lower wall impingement.

Declaration of Competing Interest

The authors declare that they have no known competing financial interests or personal relationships that could have appeared to influence the work reported in this paper.

CRediT authorship contribution statement

Aniket P. Kulkarni: Conceptualization, Investigation, Methodology, Software, Formal analysis, Writing - original draft. **Thanos Megaritis:** Conceptualization, Writing - review & editing, Formal analysis, Supervision, Resources, Funding acquisition. **Lionel Christopher Ganippa:** Conceptualization, Writing - review & editing, Supervision, Resources, Funding acquisition, Formal analysis.

Acknowledgments

The authors acknowledge the financial support of Engineering and Physical Sciences Research Council (EPSRC) of the UK under Grant No.EP/P031226/1 for this work.

References

Albonair, 2017. Albonair urea dosing system sample type lhp2-7 and lhp2-10: Quick manual for test bench applications.

Ayoub, M., Irfan, M.F., Yoo, K.-S., 2011. Surfactants as additives for NO_x reduction during sncr process with urea solution as reducing agent. Energy Convers. Manage. 52 (10), 3083–3088.

Ayyappan, P., Dou, D., Harris, T. M., 2015. Diesel exhaust fluid formulation that reduces urea deposits in exhaust systems. US Patent 8,999,277.

Birkhold, F., Meingast, U., Wassermann, P., Deutschmann, O., 2006. Analysis of the injection of urea-water-solution for automotive SCR $DeNO_x$-systems: modeling of two-phase flow and spray/wall-interaction. SAE International Journal of Engines 5 (2006-01-0643). –

Blaisot, J., Yon, J., 2005. Droplet size and morphology characterization for dense sprays by image processing: Application to the diesel spray. Exp Fluids 39 (6), 977–994.

Dörnhöfer, J., Börnhorst, M., Ates, C., Samkhaniani, N., Pfeil, J., Wörner, M., Koch, R., Bauer, H.-J., Deutschmann, O., Frohnapfel, B., et al., 2020. A holistic view on urea injection for no x emission control: impingement, re-atomization, and deposit formation. Emission Control Science and Technology 1–16.

Ebrahimian, V., Nicolle, A., Habchi, C., 2012. Detailed modeling of the evaporation and thermal decomposition of urea-water solution in SCR systems. AIChE J. 58 (7), 1998–2009.

Eggers, J., Villermaux, E., 2008. Physics of liquid jets. Rep. Prog. Phys. 71 (3), 036601.

Guan, B., Zhan, R., Lin, H., Huang, Z., 2014. Review of state of the art technologies of selective catalytic reduction of NO_x from diesel engine exhaust. Appl Therm Eng 66 (1–2), 395–414.

Guildenbecher, D., López-Rivera, C., Sojka, P., 2009. Secondary atomization. Exp Fluids 46 (3), 371.

Hopfinger, E., Lasheras, J., 1996. Explosive breakup of a liquid jet by a swirling coaxial gas jet. Physics of Fluids 8 (7), 1696–1698.

Huang, H., Chen, Y., Li, Z., Wang, H., Hao, B., Chen, Y., Lei, H., Guo, X., 2020. Analysis of deposit formation mechanism and structure optimization in urea-SCR system of diesel engine. Fuel 265, 116941.
Kapusta, Ł.J., 2017. LIF/Mie droplet sizing of water sprays from SCR system injector using structured illumination. In: ILASS2017-28th European Conference on Liquid Atomization and Spray Systems.
Kapusta, Ł.J., Sutkowski, M., Rogóż, R., Zommara, M., Teodorczyk, A., 2019. Characteristics of water and urea–water solution sprays. Catalysts 9 (9), 750.
Koebel, M., Elsener, M., Kleemann, M., 2000. Urea-SCR: A promising technique to reduce NO_x emissions from automotive diesel engines. Catal Today 59 (3–4), 335–345.
Kooij, S., Sijs, R., Denn, M.M., Villermaux, E., Bonn, D., 2018. What determines the drop size in sprays? Phys. Rev. X 8 (3), 031019.
Kulkarni, A.P., Deshmukh, D., 2017. Spatial drop-sizing in airblast atomization- An experimental study. Atomization Sprays 27 (11), 949–961.
Lasheras, J., Villermaux, E., Hopfinger, E., 1998. Break-up and atomization of a round water jet by a high-speed annular air jet. J Fluid Mech 357, 351–379.
Lecompte, M., Raux, S., Frobert, A., 2014. Experimental characterization of SCR $DeNO_x$ systems: Visualization of urea-water-solution and exhaust gas mixture. SAE Technical Paper. SAE International.
Liao, Y., 2017. Heat transfer characteristics of spray impingement in mobile selective catalytic reduction systems. ETH Zurich Ph.D. thesis..
Liao, Y., Eggenschwiler, P.D., Rentsch, D., Curto, F., Boulouchos, K., 2017. Characterization of the urea-water spray impingement in diesel selective catalytic reduction systems. Appl Energy 205, 964–975.
Lieber, C., Koch, R., Bauer, H.-J., 2019. Microscopic imaging spray diagnostics under high temperature conditions: application to urea–water sprays. Applied Sciences 9 (20), 4403.
Matas, J.-P., Cartellier, A., 2013. Flapping instability of a liquid jet. Comptes Rendus Mécanique 341 (1–2), 35–43.
Needham, D., Spadafora, P., Schiffgens, H., Kirwan, J., Cabush, D., Kalina, A., 2012. Delphi SCR dosing system-an alternative approach for close-coupled SCR catalyst systems. In: SIA Diesel International Conference, Rouen.
Oh, J., Lee, K., 2014. Spray characteristics of a urea solution injector and optimal mixer location to improve droplet uniformity and NO_x conversion efficiency for selective catalytic reduction. Fuel 119, 90–97.
Payri, R., Bracho, G., Gimeno, J., Moreno, A., 2019. Investigation of the urea-water solution atomization process in engine exhaust-like conditions. Exp. Therm Fluid Sci. 108, 75–84.
Payri, R., Bracho, G., Gimeno, J., Moreno, A., 2019. Spray Characterization of the Urea-Water Solution UWS Injected in a Hot Air Stream Analogous to SCR System Operating Conditions. Technical Report. SAE Technical Paper.
Postrioti, L., Brizi, G., Ungaro, C., Mosser, M., Bianconi, F., 2015. A methodology to investigate the behaviour of urea-water sprays in high temperature air flow for SCR de- NO_x applications. Fuel 150, 548–557.
Pratama, R.H., Moon, S., Kim, H.-H., Oguma, M., 2019. Application of electrostatic force for the atomization improvement of urea-water sprays in diesel SCR systems. Fuel 116571.
Rajamanickam, K., Basu, S., 2017. Insights into the dynamics of spray–swirl interactions. J Fluid Mech 810, 82–126.
Ruiz, C.C., 1999. Micelle formation and microenvironmental properties of sodium dodecyl sulfate in aqueous urea solutions. Colloids Surf., A 147 (3), 349–357.
Shi, X., Deng, J., Wu, Z., Li, L., 2013. Effect of injection parameters on spray characteristics of urea-SCR system. SAE Int. J. Engines 6 (2), 873–881.
Sijs, R., Bonn, D., 2020. The effect of adjuvants on spray droplet size from hydraulic nozzles. Pest Manag. Sci..
Sijs, R., Kooij, S., Bonn, D., 2019. How surfactants influence the drop size in sprays. arXiv preprint arXiv:1907.09723.
Spiteri, A., Eggenschwiler, P.D., Liao, Y., Wigley, G., Michalow-Mauke, K.A., Elsener, M., Kröcher, O., Boulouchos, K., 2015. Comparative analysis on the performance of pressure and air-assisted urea injection for selective catalytic reduction of NO_x. Fuel 161, 269–277.
Tareq, M.M., Jung, R.A.D.S., Lee, J., 2020. Effect of the physical properties of liquid and alr on the spray characteristics of a pre-filming airblast nozzle. Int. J. Multiphase Flow 103240.
Varga, C.M., Lasheras, J.C., Hopfinger, E.J., 2003. Initial breakup of a small-diameter liquid jet by a high-speed gas stream. J Fluid Mech 497, 405–434.
Varna, A., Spiteri, A.C., Wright, Y.M., Eggenschwiler, P.D., Boulouchos, K., 2015. Experimental and numerical assessment of impingement and mixing of urea–water sprays for nitric oxide reduction in diesel exhaust. Appl Energy 157, 824–837.
Wasow, G., Strutz, E. O., 2015. Method for minimizing the diameter of a urea solution, urea solution and use of a surfactant in urea solution. US Patent 9,050,560 B2.
Wong, D., Simmons, M., Decent, S., Parau, E., King, A., 2004. Break-up dynamics and drop size distributions created from spiralling liquid jets. Int. J. Multiphase Flow 30 (5), 499–520.
Zhao, H., Wu, Z.-W., Li, W.-F., Xu, J.-L., Liu, H.-F., 2018. Transition weber number between surfactant-laden drop bag breakup and shear breakup of secondary atomization. Fuel 221, 138–143.
Zheng, G., 2017. Development of Air-Assisted Urea Injection Systems for Medium Duty Trucks. Technical Report. SAE Technical Paper.